

pubs.acs.org/JPCL Letter

Origin of the near 400 nm Absorption and Emission Band in the Synthesis of Cesium Lead Bromide Nanostructures: Metal Halide Molecular Clusters Rather Than Perovskite Magic-Sized Clusters

Allison A. Win, Kai-Chun Chou, David C. Zeitz, Celia Todd, and Jin Z. Zhang*



Cite This: J. Phys. Chem. Lett. 2023, 14, 116-121



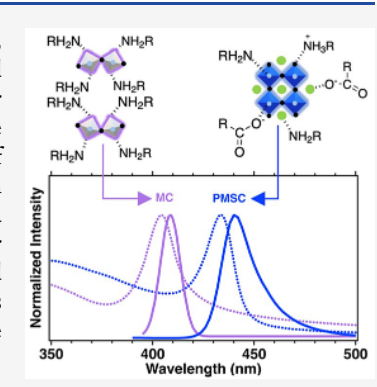
ACCESS

III Metrics & More

Article Recommendations

Supporting Information

ABSTRACT: In the synthesis of cesium lead bromide (CsPbBr₃) perovskite quantum dots, with an electronic absorption and emission band around 510 nm, and perovskite magic-sized clusters (PMSCs), with an electronic absorption and emission band around 430 nm, another distinct absorption and emission around 400 nm is often observed. While many would attribute this band to small perovskite particles, here we show strong evidence that this band is a result of the formation of lead bromide molecular clusters (PbBr₂ MCs) passivated with ligands, which do not contain the A component of the ABX₃ perovskite structure. This evidence comes from a systematic comparative study of the reaction products with and without the A component under otherwise identical experimental conditions. The results support that the near 400 nm band originates from ligand-passivated PbBr₂ MCs. This observation seems to be quite general and is significant in understanding the nature of the reaction products in the synthesis of metal halide perovskite nanostructures.



erovskite quantum dots (PQDs) are semiconductor nanoparticles defined by the ABX3 formula, where A is an inorganic or organic cation (Cs⁺ or CH₃NH₃⁺), B is a metal cation (Pb2+), and X is a halide anion (Cl-, Br-, I-). They exhibit coveted properties such as narrow emission bands and a tunable emission across the visible spectrum. 1-5 The tunable properties of PQDs are attributed to the quantum confinement effect and a large surface-to-volume ratio, and can be manipulated through altering the crystal size or halide composition. 6-9 CsPbBr₃ PQDs, in particular, are of increased interest due to a near-unity photoluminescence (PL) quantum yield as well as its facile and inexpensive synthesis and high PL quantum yield. 10,11 These nanoparticles are characterized by a bright green fluorescence under ultraviolet excitation, with an absorption band at around 505 nm and an emission band at around 516 nm. 12,13 While exploring the manipulation of the optical properties of CsPbBr3 PQDs, perovskite magic-sized clusters were introduced. 14-1

Perovskite magic-sized clusters (PMSCs) are smaller and narrower than conventional PQDs and are characterized by discrete size distributions and sharp absorption and emission peaks. ^{13,14,16,18–26} They are often described as stable intermediates to PQDs or bulk perovskites, making them ideal models for understanding the growth mechanism of PMSCs to larger perovskite nanomaterials. ¹⁷ This synergistic relationship was showcased when Xu et al. demonstrated the tuning of cesium lead bromide (CsPbBr₃) PQDs to PMSCs through the addition of a trivalent metal hydrated nitrate coordination complex (TMHNCC) in conjunction with conventional passivating ligands, oleic acid, and oleylamine.

These CsPbBr₃ PMSCs exhibited a monodispersed excitonic absorption peak at 413 nm and PL emission peak at 421 nm.¹⁴ A subsequent paper by Xu et al. presented a tuning of CsPbBr₃ PMSCs by controlling the ratio of carboxylic acids with benzylamine, wherein the characteristic CsPbBr₃ PMSC excitonic absorption peak and PL emission peak were reported to be between 389 to 399 nm and 391 to 402 nm, respectively.¹⁵ While exploring the growth mechanism of PMSCs to PQDs, lead bromide molecular clusters (MCs) were found as a potential precursor to PMSCs.¹⁷

Lead bromide molecular clusters (PbBr₂ MCs) exhibit similar optical properties to PMSCs, such as bluer and narrower excitonic absorption and emission peaks and single size distributions. ^{1,17,27–29} However, PbBr₂ MCs lack the perovskite composition since they have no A component. PbBr₂ MCs also only require an amine to passivate its structure, though adding an acid does not drastically change the product's composition or optical properties. Vickers et al. demonstrated that PbBr₂ MCs are a potential precursor to PMSCs and that, given the appropriate experimental conditions, PMSCs can revert back to PbBr₂ MCs after a period of time. ¹⁷ However, the reported absorption and

Received: December 8, 2022 Accepted: December 22, 2022



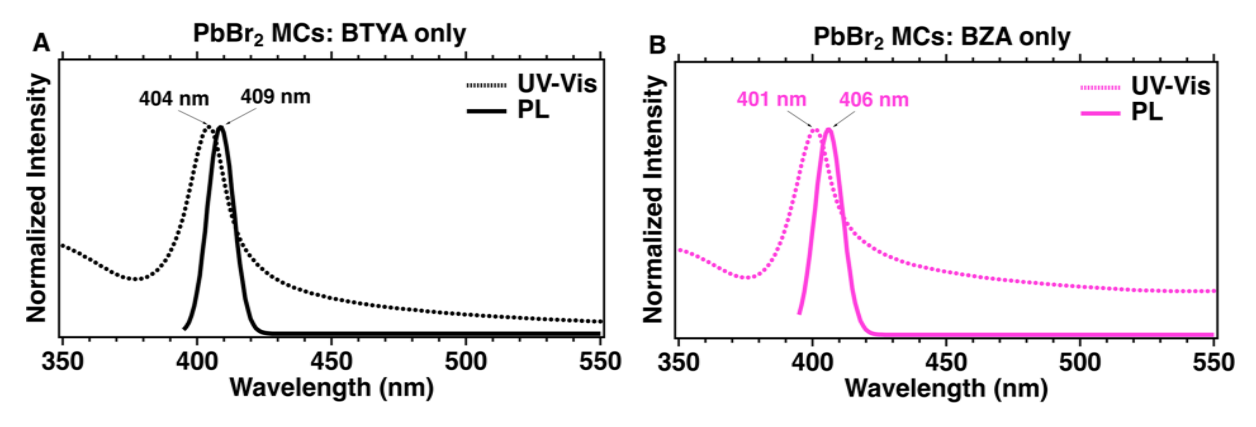


Figure 1. UV-vis absorption and PL spectra of (a) BTYA PbBr₂ and (b) BZA PbBr₂.

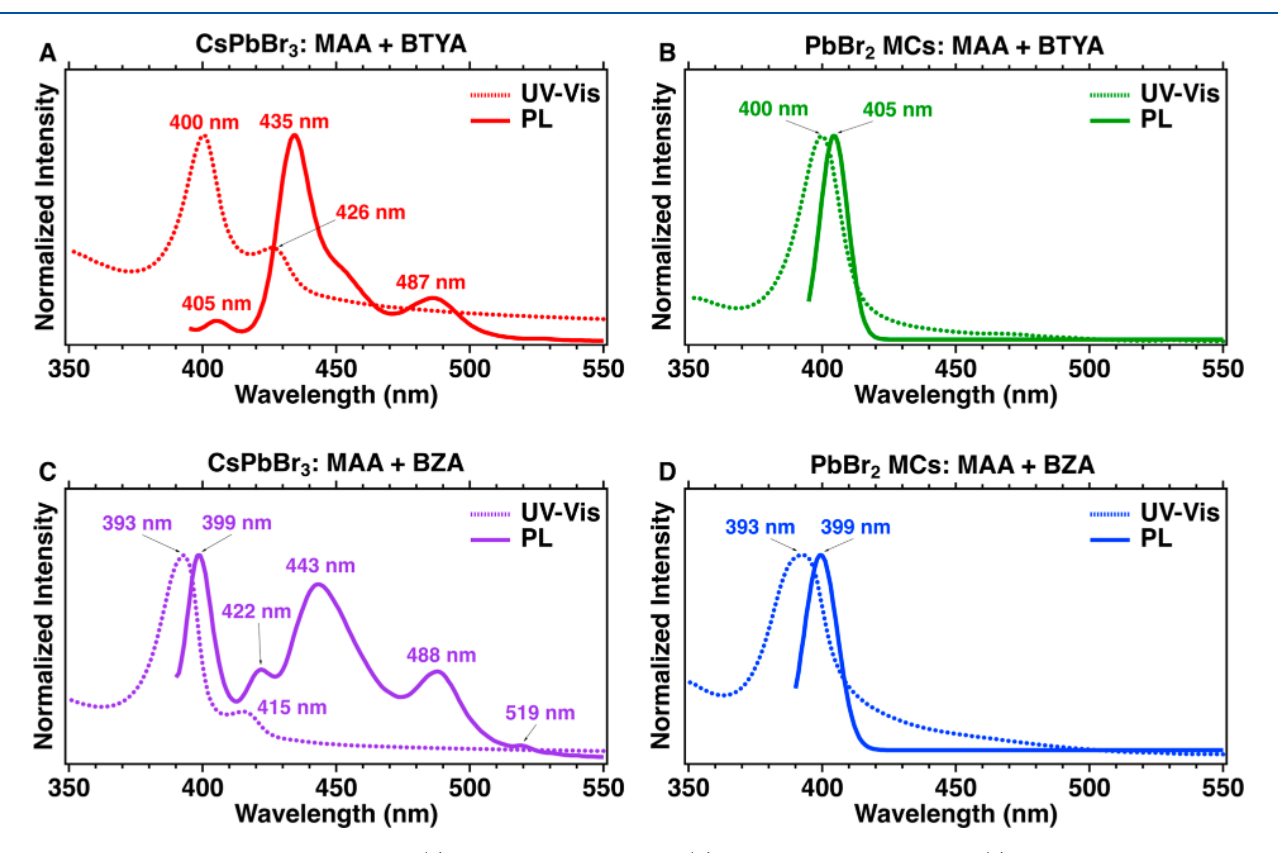


Figure 2. UV—vis absorption and PL spectra of (a) MAA + BTYA CsPbBr₃, (b) MAA + BTYA PbBr₂ MCs, (c) MAA + BZA CsPbBr₃, and (d) MAA + BZA PbBr₂ MCs.

emission for PbBr₂ MCs passivated with butylamine are respectively around 400 and 410 nm, which overlaps with the already established CsPbBr₃ PMSCs. Furthermore, a comparison between MCs and PMSCs was limited to PbBr₂ MCs and methylammonium lead bromide PMSCs, which have established absorption and emission bands at around 420 and 430 nm, respectively, but did not explore the synergistic relationship with CsPbBr₃ PMSCs. ^{1,2,16,17,24,31} Due to the equilibrium of these two species and the fact that PbBr₂ MCs were identified after preliminary publications on PMSCs, it is important to clarify the origin of the 400 nm absorption peak so that future classifications are not jeopardized.

In this study, we perform a series of comparison experiments where we synthesize CsPbBr₃ nanoparticles with and without the cesium component through ligand-assisted reprecipitation (LARP), using different organic ligands to passivate the

nanoparticles. These ligands were used in previously established protocols for synthesizing perovskite nanoparticles, focusing on carboxylic acids like mesitylacetic acid (MAA), valeric acid (VA), and octanoic acid (OcA), as well as organic amines like butylamine (BTYA) and benzylamine (BZA). ^{1,2,13-17,21,24,27,29,31-33,30} Other organic acids used for passivation include oleic acid (OA), benzoic acid (BA), and phenylacetic acid (PAA). PbBr₂ MCs were found to have formed in all of the tested conditions and tend to absorb and emit at wavelengths that were previously attributed to CsPbBr₃ PMSCs. These results suggest that what our group has earlier characterized as CsPbBr₃ PMSCs are PbBr₂ MCs and further establish the presumption that PbBr₂ MCs are an important precursor in the reaction dynamics of perovskite nanoparticles.

Figure 1A and B show the ultraviolet-visible (UV-vis) electronic absorption and PL spectra of PbBr₂ MCs passivated

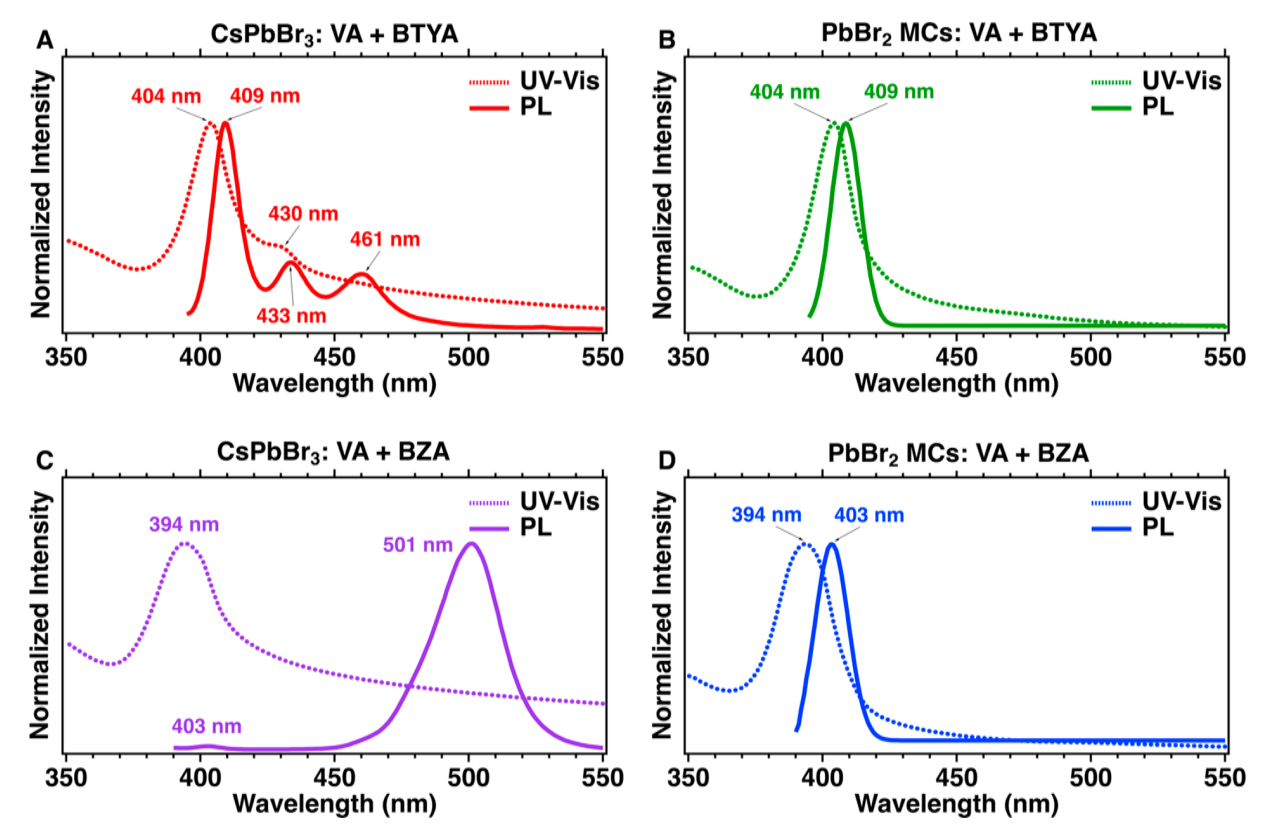


Figure 3. UV—vis absorption and PL spectra of (a) VA + BTYA CsPbBr₃, (b) VA + BTYA PbBr₂ MCs, (c) VA + BZA CsPbBr₃, and (d) VA + BZA PbBr₂ MCs.

with BTYA and BZA, respectively. BTYA PbBr₂ MCs have an electronic absorption band peak at 404 nm and emission band peak at 409 nm, which are consistent with the values reported by Vickers et al.¹⁷ BZA PbBr₂ MCs have an electronic absorption band at 401 nm and an emission band at 406 nm, indicating that PbBr₂ MCs passivated with BZA are slightly smaller than their BTYA counterpart. These values serve as a reference for PbBr₂ MCs in terms of where they absorb and emit in subsequent comparative studies.

Figure 2A shows the UV-vis absorption and PL emission spectra of CsPbBr3 nanoparticle passivation with MAA and BTYA. These MAA+BTYA CsPbBr3 nanoparticles have two excitonic absorption bands at 400 and 426 nm, and three PL emission bands at 405, 435, and 487 nm. The multiple emission is a result of the quantum size effect, which affects the number of layers of the perovskite nanoparticles. A difference in the number of layers results in varied emission on the PL spectra. 34,35 Figure 2B shows the UV-vis absorption and PL spectra of PbBr₂ MCs passivated with MAA and BTYA, lacking the cesium component that would complete the perovskite structure. These MAA + BTYA PbBr₂ MCs have an electronic absorption band peak at 400 nm and emission band peak at 405 nm. The high similarity in the near 400 nm absorption and PL bands between the two samples, with and without the Cs⁺ component, strongly implies that the near 400 nm bands in Figure 2A originate from PbBr₂ MCs^{13,17,27,29} and not from PMSCs. The 426 nm absorption and 435 nm emission bands can be attributed to CsPbBr₃ PMSCs, ^{14–17,21,24,25,31} while the 487 nm emission band is most likely due to a small amount of CsPbBr₃ PQDs with a high photoluminescence quantum yield (PLQY) or trap states in the structure. 3,8,10,12,18,36

Figure 2C shows the UV-vis absorption and PL emission spectra of CsPbBr3 nanoparticles passivated with MAA and BZA. These MAA + BZA perovskite nanoparticles have two distinct excitonic peaks at 393 and 415 nm but several emission peaks at 399, 422, 443, 488, and 519 nm. Figure 2D shows the UV-vis absorption and PL emission spectra of the sample synthesized under the same conditions except without Cs⁺ added, which exhibit an absorption band peak at 393 nm and an emission band peak at 399 nm attributed to MAA + BZA PbBr₂ MCs. ^{13,17,27,29} The absorption and emission peaks for the MCs without Cs⁺ match those of the nanoparticles with the Cs⁺ component present, which suggest that the near 400 nm bands in Figure 2C originate from PbBr₂ MCs formed in the synthesis of CsPbBr₃ nanoparticles. The 422 and 443 nm emission peaks are attributed to $CsPbBr_3$ PMSCs $^{14-17,21,24,25,31}$ and the 488 nm and 494 nm emissions to CsPbBr₃ PQDs. 3,8,10,12,18,36

Figure 3A shows the UV—vis absorption and PL emission spectra of CsPbBr₃ nanoparticles passivated with VA and BTYA. This condition also renders two electronic absorption bands at 404 and 430 nm and multiple PL emission bands at 409, 433, and 461 nm. Figure 3B shows the UV—vis absorption and PL emission spectra of the sample synthesized similarly without Cs⁺, with an absorption band at 404 nm and emission band at 409 nm, which can be attributed to VA+BTYA PbBr₂ MCs. ^{13,17,27,29} As before, the overlapping absorption and emission bands of the approximate 400 nm peaks regardless of the presence of Cs⁺ suggest that PbBr₂ MCs are responsible for the 404 nm absorption band and 409 nm emission band observed in Figure 3A for the sample with Cs⁺ present. The 433 nm emission band is due to CsPbBr₃

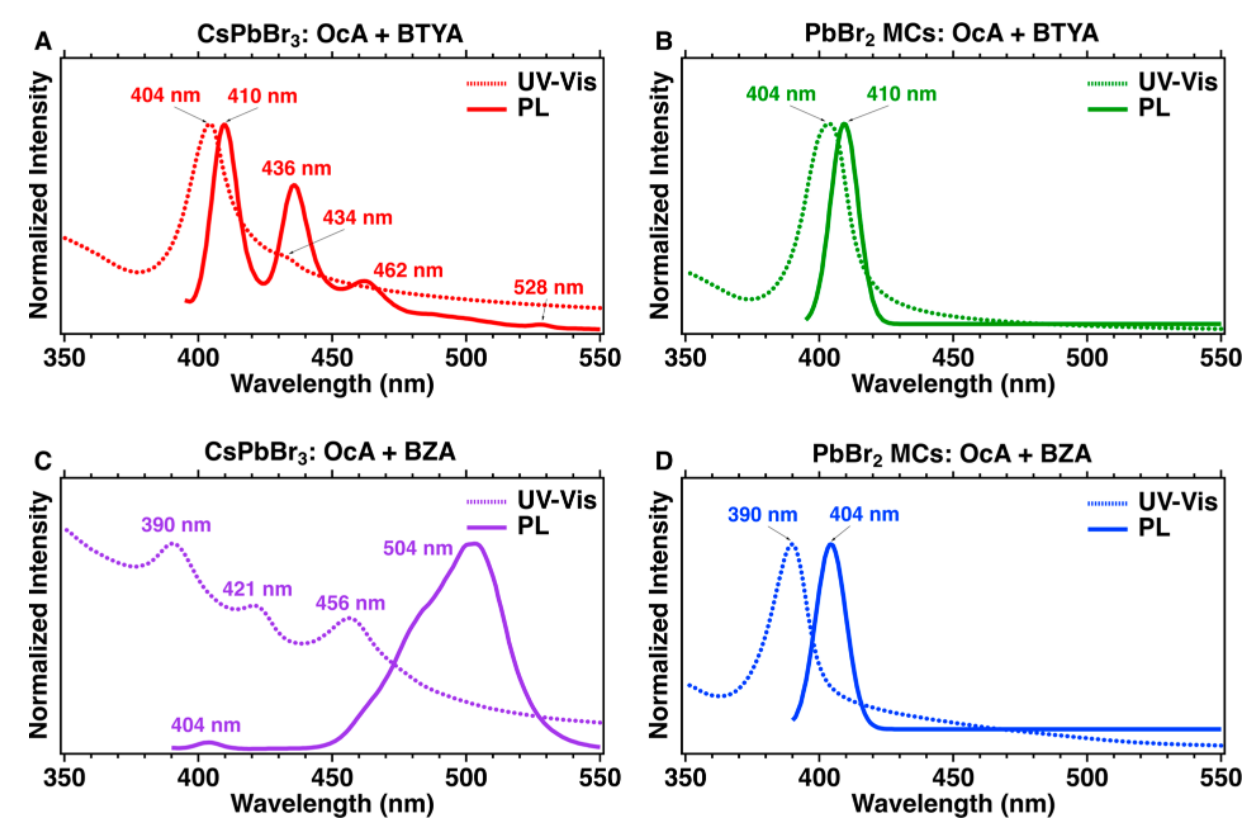


Figure 4. UV—vis absorption and PL spectra of (a) OcA + BTYA CsPbBr₃, (b) OcA + BTYA PbBr₂ MCs, (c) OcA + BZA CsPbBr₃, and (d) OcA + BZA PbBr₂ MCs.

PMSCs, $^{14-17,21,24,25,31}$ and the 461 nm emission peak is from small CsPbBr $_3$ PQDs or trap states. 3,8,10,12,18,36

Figure 3C shows the UV—vis absorption and PL emission spectra of CsPbBr3 nanoparticles passivated with VA and BZA. These nanoparticles are represented by one broad electronic peak at 393 nm, and two emission bands at 403 and 501 nm. Figure 3D shows the absorption and emission spectra under the same conditions but without the Cs⁺ component, with an absorption band peak at 394 nm and an emission band at 403 nm. Because of the overlap of the 394 nm absorption band and the 403 nm emission band with and without the presence of Cs⁺, we attribute the 394 nm absorption band and the 403 nm emission band to PbBr₂ MCs seen in Figure 3C for the sample with Cs⁺ present. ^{13,17,27,29} The 501 nm emission band is most likely attributed to CsPbBr₃ PQDs with a high PLQY, which may contribute to the low intensity of the PbBr₂ MCs. ^{3,8,10,12,18,36}

Figure 4A depicts the UV—vis absorption and PL emission spectra of CsPbBr₃ nanoparticles passivated with OcA and BTYA. These nanoparticles are characterized by a single strong absorption band at 404 nm and a broader absorption band at 434 nm, as well as several emission peaks at 410, 436, 462, and 528 nm. Figure 4B shows the absorption and PL spectra of samples synthesized under almost identical conditions except without Cs⁺, with an absorption band at 404 nm and an emission band peaked at 410 nm attributed to OcA + BTYA PbBr₂ MCs. ^{13,17,27,29} The consistent overlap makes it reasonable to assume that the 404 nm absorption peak and the 410 nm emission peak in Figure 4A are due to PbBr₂ MCs. The 436 nm emission band is attributed to CsPbBr₃ PMSCs. ^{14–17,21,24,25,31} The 462 nm emission band is from

small CsPbBr₃ PQDs or trap states, and the 528 nm emission band is from CsPbBr₃ PQDs. ^{3,8,10,12,18,36}

The UV-vis absorption and PL emission spectra for CsPbBr₃ nanoparticles passivated with OcA and BZA are shown in Figure 4C. The product has three excitonic species at 390, 421, and 456 nm, and two emissive species at 404 and 504 nm. When the synthesis was carried out without the Cs⁺ component, the absorption and PL spectra shown in Figure 4D exhibit an absorption band at 390 nm and emission band at 404 nm. This again supports that the species that absorbs at 390 nm and emits at 404 nm in Figure 4C is PbBr₂ MCs even with the presence of Cs⁺. ¹³, ¹⁷, ²⁷, ²⁹ There is a notable lack of CsPbBr₃ PMSCs in the emission spectra but a clear indication of its presence in the absorption spectra at 421 nm, likely due to self-absorption of the emission spectra at 421 nm, likely due to self-absorption of the emission spectra at 421 nm emission band can be attributed to CsPbBr₃ PQDs. ^{3,8,10,12,18,36}

Compared to the PL band at 400 nm for PbBr₂ MCs in Figure 2 with MAA + BZA and MAA + BTYA as the passivating ligands, the 403 nm emission band in Figure 3C with VA + BZA as ligands and the 404 nm emission band in Figure 4C with OcA + BZA as ligands are relatively weaker. A weaker PL is usually attributed to a higher density of defects or less effective passivation. The above comparison shows the following trend: ligand pairs that are "similar" (straight-chain acid with straight-chain amine or aromatic acid with aromatic amine) favor the PbBr₂ MC formation, whereas "mixed" ligand pairs (straight-chain acid with aromatic amine or vice versa) seem to favor the formation of PQDs or PMSCs. We suggest that this is possibly due to similar ligands being more ordered compared to mixed ligands, and more ordered ligands lead to better passivation, lower density of defects, and the formation

of MCs. Previous studies have already found that MCs need better passivation than PQDs or PMSCs. 13,17,27,29

Even though this work does not focus on determination of the structure of the MCs, we suggest that the MCs have layered structures based on our previous study from our lab²⁹ and related work from others. ^{34,35} If the proposed layered structure is correct, then the MCs represent ultrasmall "quantum well in quantum dot" structures.

In summary, through a series of control experiments, we have demonstrated the synthesis of ligand-passivated PbBr₂ MCs with a strong absorption and PL emission band near 400 nm with and without the A (Cs⁺) component of perovskites under otherwise identical experimental conditions. Comparative UV—vis and PL spectroscopic characterizations show convincingly that the 400 nm band is due to ligand-passivated PbBr₂ MCs rather than CsPbBr₃ PMSCs as one may expect when Cs⁺ is present in the synthesis. The CsPbBr₃ PMSCs absorb around 420 to 440 nm and emit around 426 to 450 nm. Clarification of the origin of the near 400 nm band in the synthesis of metal halide perovskites is important in understanding the mechanism of synthesis of nanostructures of metal halide perovskites.

ASSOCIATED CONTENT

5 Supporting Information

The Supporting Information is available free of charge at https://pubs.acs.org/doi/10.1021/acs.jpclett.2c03734.

Details of materials and synthesis and extra spectroscopic measurements (UV-vis absorption, photoluminescence) for further comparisons of different organic ligands with and without the cesium component (PDF)

AUTHOR INFORMATION

Corresponding Author

Jin Z. Zhang — Department of Chemistry and Biochemistry, University of California, Santa Cruz, California 95064, United States; orcid.org/0000-0003-3437-912X; Phone: +1-831-459-3776; Email: zhang@ucsc.edu

Authors

Allison A. Win — Department of Chemistry and Biochemistry, University of California, Santa Cruz, California 95064, United States; orcid.org/0000-0001-7867-1953

Kai-Chun Chou – Department of Chemistry and Biochemistry, University of California, Santa Cruz, California 95064, United States

David C. Zeitz – Department of Chemistry and Biochemistry, University of California, Santa Cruz, California 95064, United States

Celia Todd – Department of Chemistry and Biochemistry, University of California, Santa Cruz, California 95064, United States

Complete contact information is available at: https://pubs.acs.org/10.1021/acs.jpclett.2c03734

Notes

The authors declare no competing financial interest.

ACKNOWLEDGMENTS

J.Z.Z. acknowledges financial support by National Science Foundation (CHE-2203633). A.A.W. and D.C.Z. are grateful

to the QB3-UCSC Fellowship for Interdisciplinary Excellence for financial support.

REFERENCES

- (1) Dey, A.; Ye, J.; De, A.; Debroye, E.; Ha, S. K.; Bladt, E.; Kshirsagar, A. S.; Wang, Z.; Yin, J.; Wang, Y.; Quan, L. N.; et al. State of the Art and Prospects for Halide Perovskite Nanocrystals. *ACS Nano* **2021**, *15* (7), 10775–10981.
- (2) Zhang, J. Z. A Cocktail" Approach to Effective Surface Passivation of Multiple Surface Defects of Metal Halide Perovskites Using a Combination of Ligands. *J. Phys. Chem. Lett.* **2019**, *10* (17), 5055–5063.
- (3) Wang, H.-C.; Bao, Z.; Tsai, H.-Y.; Tang, A.-C.; Liu, R.-S. Perovskite Quantum Dots and Their Application in Light-Emitting Diodes. *Small* **2018**, *14* (1), 1702433.
- (4) Li, G.; Huang, J.; Zhu, H.; Li, Y.; Tang, J.-X.; Jiang, Y. Surface Ligand Engineering for Near-Unity Quantum Yield Inorganic Halide Perovskite QDs and High-Performance QLEDs. *Chem. Mater.* **2018**, 30 (17), 6099–6107.
- (5) Park, J. H.; Lee, A.; Yu, J. C.; Nam, Y. S.; Choi, Y.; Park, J.; Song, M. H. Surface Ligand Engineering for Efficient Perovskite Nanocrystal-Based Light-Emitting Diodes. ACS Appl. Mater. Interfaces 2019, 11 (8), 8428–8435.
- (6) Chen, X.; Peng, L.; Huang, K.; Shi, Z.; Xie, R.; Yang, W. Non-Injection Gram-Scale Synthesis of Cesium Lead Halide Perovskite Quantum Dots with Controllable Size and Composition. *Nano Res.* **2016**, *9* (7), 1994–2006.
- (7) Leng, J.; Wang, T.; Zhao, X.; Ong, E. W. Y.; Zhu, B.; Ng, J. D. A.; Wong, Y.-C.; Khoo, K. H.; Tamada, K.; Tan, Z.-K. Thermodynamic Control in the Synthesis of Quantum-Confined Blue-Emitting CsPbBr3 Perovskite Nanostrips. *J. Phys. Chem. Lett.* **2020**, *11* (6), 2036–2043.
- (8) Dong, Y.; Qiao, T.; Kim, D.; Parobek, D.; Rossi, D.; Son, D. H. Precise Control of Quantum Confinement in Cesium Lead Halide Perovskite Quantum Dots via Thermodynamic Equilibrium. *Nano Lett.* **2018**, *18* (6), 3716–3722.
- (9) Tyagi, P.; Arveson, S. M.; Tisdale, W. A. Colloidal Organohalide Perovskite Nanoplatelets Exhibiting Quantum Confinement. *J. Phys. Chem. Lett.* **2015**, *6* (10), 1911–1916.
- (10) Zhao, Y.; Li, J.; Dong, Y.; Song, J. Synthesis of Colloidal Halide Perovskite Quantum Dots/Nanocrystals: Progresses and Advances. *Isr. J. Chem.* **2019**, *59* (8), 649–660.
- (11) Tsai, H.; Asadpour, R.; Blancon, J.-C.; Stoumpos, C. C.; Durand, O.; Strzalka, J. W.; Chen, B.; Verduzco, R.; Ajayan, P. M.; Tretiak, S.; et al. D. Light-Induced Lattice Expansion Leads to High-Efficiency Perovskite Solar Cells. *Science* **2018**, *360* (6384), 67–70.
- (12) Li, X.; Wu, Y.; Zhang, S.; Cai, B.; Gu, Y.; Song, J.; Zeng, H. CsPbX3 Quantum Dots for Lighting and Displays: Room-Temperature Synthesis, Photoluminescence Superiorities, Underlying Origins and White Light-Emitting Diodes. *Adv. Funct. Mater.* **2016**, *26* (15), 2435–2445.
- (13) Liu, L.; Pan, K.; Xu, K.; Zhang, J. Z. Impact of Molecular Ligands in the Synthesis and Transformation between Metal Halide Perovskite Quantum Dots and Magic Sized Clusters. *ACS Phys. Chem. Au* **2022**, *2* (3), 156–170.
- (14) Xu, K.; Allen, A. C.; Luo, B.; Vickers, E. T.; Wang, Q.; Hollingsworth, W. R.; Ayzner, A. L.; Li, X.; Zhang, J. Z. Tuning from Quantum Dots to Magic Sized Clusters of CsPbBr3 Using Novel Planar Ligands Based on the Trivalent Nitrate Coordination Complex. J. Phys. Chem. Lett. 2019, 10 (15), 4409–4416.
- (15) Xu, K.; Vickers, E. T.; Luo, B.; Wang, Q.; Allen, A. C.; Wang, H.; Cherrette, V.; Li, X.; Zhang, J. Z. Room Temperature Synthesis of Cesium Lead Bromide Perovskite Magic Sized Clusters with Controlled Ratio of Carboxylic Acid and Benzylamine Capping Ligands. Sol. Energy Mater. Sol. Cells 2020, 208, 110341.
- (16) Liu, L.; Xu, K.; Vickers, E. T.; Allen, A.; Li, X.; Peng, L.; Zhang, J. Z. Varying the Concentration of Organic Acid and Amine Ligands Allows Tuning between Quantum Dots and Magic-Sized Clusters of

- CH3NH3PbBr3 Perovskite: Implications for Photonics and Energy Conversion. ACS Appl. Nano Mater. 2020, 3 (12), 12379-12387.
- (17) Vickers, E. T.; Chen, Z.; Cherrette, V.; Smart, T.; Zhang, P.; Ping, Y.; Zhang, J. Z. Interplay between Perovskite Magic-Sized Clusters and Amino Lead Halide Molecular Clusters. Research 2021, 2021.1
- (18) Evans, C. M.; Love, A. M.; Weiss, E. A. Surfactant-Controlled Polymerization of Semiconductor Clusters to Quantum Dots through Competing Step-Growth and Living Chain-Growth Mechanisms. J. Am. Chem. Soc. 2012, 134 (41), 17298-17305.
- (19) Yu, K. CdSe Magic-Sized Nuclei, Magic-Sized Nanoclusters and Regular Nanocrystals: Monomer Effects on Nucleation and Growth. Adv. Mater. 2012, 24 (8), 1123-1132.
- (20) Nevers, D. R.; Williamson, C. B.; Savitzky, B. H.; Hadar, I.; Banin, U.; Kourkoutis, L. F.; Hanrath, T.; Robinson, R. D. Mesophase Formation Stabilizes High-Purity Magic-Sized Clusters. J. Am. Chem. Soc. 2018, 140 (10), 3652-3662.
- (21) Xu, K.; Vickers, E. T.; Luo, B.; Allen, A. C.; Chen, E.; Roseman, G.; Wang, Q.; Kliger, D. S.; Millhauser, G. L.; Yang, W.; et al. First Synthesis of Mn-Doped Cesium Lead Bromide Perovskite Magic Sized Clusters at Room Temperature. J. Phys. Chem. Lett. 2020, 11 (3), 1162-1169.
- (22) Peng, L.; Dutta, A.; Xie, R.; Yang, W.; Pradhan, N. Dot-Wire-Platelet-Cube: Step Growth and Structural Transformations in CsPbBr3 Perovskite Nanocrystals. ACS Energy Lett. 2018, 3 (8), 2014-2020.
- (23) Xu, Y.; Zhang, Q.; Lv, L.; Han, W.; Wu, G.; Yang, D.; Dong, A. Synthesis of Ultrasmall CsPbBr3 Nanoclusters and Their Transformation to Highly Deep-Blue-Emitting Nanoribbons at Room Temperature. Nanoscale 2017, 9 (44), 17248-17253.
- (24) Vickers, E. T.; Xu, K.; Dreskin, B. W.; Graham, T. A.; Li, X.; Zhang, J. Z. Ligand Dependent Growth and Optical Properties of Hybrid Organo-Metal Halide Perovskite Magic Sized Clusters. J. Phys. Chem. C 2019, 123 (30), 18746-18752.
- (25) Palencia, C.; Yu, K.; Boldt, K. The Future of Colloidal Semiconductor Magic-Size Clusters. ACS Nano 2020, 14 (2), 1227-
- (26) Harrell, S. M.; McBride, J. R.; Rosenthal, S. J. Synthesis of Ultrasmall and Magic-Sized CdSe Nanocrystals. Chem. Mater. 2013, 25 (8), 1199-1210.
- (27) Liu, L.; Pan, K.; Xu, K.; Peng, X.; Zhang, J. Z. Synthesis and Optical Properties of Mn2+-Doped Amino Lead Halide Molecular Clusters Assisted by Chloride Ion. J. Phys. Chem. Lett. 2021, 12 (31), 7497-7503.
- (28) Zhou, C.; Lin, H.; Worku, M.; Neu, J.; Zhou, Y.; Tian, Y.; Lee, S.; Djurovich, P.; Siegrist, T.; Ma, B. Blue Emitting Single Crystalline Assembly of Metal Halide Clusters. J. Am. Chem. Soc. 2018, 140 (41), 13181-13184.
- (29) Zhang, H.; Vickers, E. T.; Erickson, S.; Guarino-Hotz, M.; Barnett, J. L.; Ghosh, S.; Zhang, J. Z. Synthesis and Properties of Stable Amino Metal Halide Molecular Clusters in the Solid State. J. Phys. Chem. Lett. 2022, 13 (45), 10543-10549.
- (30) Guarino-Hotz, M.; Barnett, J. L.; Pham, L. B.; Win, A. A.; Cherrette, V. L.; Zhang, J. Z. Tuning between Methylammonium Lead Bromide Perovskite Magic-Sized Clusters and Quantum Dots through Ligand Assisted Reprecipitation at Elevated Temperatures. J. Phys. Chem. C 2022, 126 (32), 13854-13862.
- (31) Luo, B.; Li, F.; Xu, K.; Guo, Y.; Liu, Y.; Xia, Z.; Zhang, J. Z. B-Site Doped Lead Halide Perovskites: Synthesis, Band Engineering, Photophysics, and Light Emission Applications. J. Mater. Chem. C **2019**, 7 (10), 2781–2808.
- (32) Liu, L.; Xu, K.; Allen, A. L.; Li, X.; Xia, H.; Peng, L.; Zhang, J. Z. Enhancing the Photoluminescence and Stability of Methylammonium Lead Halide Perovskite Nanocrystals with Phenylalanine. J. Phys. Chem. C 2021, 125 (4), 2793–2801.
- (33) Luo, B.; Pu, Y.-C.; Lindley, S. A.; Yang, Y.; Lu, L.; Li, Y.; Li, X.; Zhang, J. Z. Organolead Halide Perovskite Nanocrystals: Branched Capping Ligands Control Crystal Size and Stability. Angew. Chem., Int. Ed. 2016, 55 (31), 8864-8868.

- (34) Weidman, M. C.; Goodman, A. J.; Tisdale, W. A. Colloidal Halide Perovskite Nanoplatelets: An Exciting New Class of Semiconductor Nanomaterials. Chem. Mater. 2017, 29 (12), 5019-
- (35) Sichert, J. A.; Tong, Y.; Mutz, N.; Vollmer, M.; Fischer, S.; Milowska, K. Z.; García Cortadella, R.; Nickel, B.; Cardenas-Daw, C.; Stolarczyk, J. K.; Urban, A. S.; Feldmann, J. Quantum Size Effect in Organometal Halide Perovskite Nanoplatelets. Nano Lett. 2015, 15 (10), 6521-6527.
- (36) C. G., S.; Jyothi, M. S.; Balakrishna, R. G. Stabilization of CsPbBr 3 Quantum Dots for Photocatalysis, Imaging and Optical Sensing in Water and Biological Medium: A Review. J. Mater. Chem. C **2022**, 10 (18), 6935–6956.

□ Recommended by ACS

Cubic Halide Double Perovskite Nanocrystals with Anisotropic Free Excitons and Self-Trapped Exciton Photoluminescence

Chao Wang, Guangjiu Zhao, et al.

DECEMBER 29, 2022

THE JOURNAL OF PHYSICAL CHEMISTRY LETTERS

READ **C**

Electronic State Modulation by Large A-Site Cations in Quasi-Two-Dimensional Organic-Inorganic Lead Halide Perovskites

Jiakai Yan, Yue Hu, et al.

DECEMBER 27, 2022

CHEMISTRY OF MATERIALS

READ 1

Self-Trapped Excitons Mediated Energy Transfer to Sm³⁺ in Cs₂AgIn_(1-x)Sm_xCl₆:Bi Double Perovskite Nanocrystals

, Sameer Sapra, et al.

DECEMBER 28, 2022

THE JOURNAL OF PHYSICAL CHEMISTRY C

READ 🗹

Stereoelectronic Effect from B-Site Dopants Stabilizes Black Phase of CsPbI,

Pimsuda Pansa-Ngat, Oleksandr Voznyy, et al.

DECEMBER 19, 2022

CHEMISTRY OF MATERIALS

READ **C**

Get More Suggestions >